Probing the Binding Domain of the NK2 Receptor with Fluorescent Ligands: Evidence That Heptapeptide Agonists and Antagonists Bind Differently

Gerardo Turcatti,[‡] Horst Vogel,[§] and André Chollet*[,‡]

Glaxo Institute for Molecular Biology, Chemin des Aulx 14, CH-1228 Geneva, Switzerland, and EPFL, Institut de Chimie-Physique, CH-1015 Lausanne, Switzerland

Received November 7, 1994; Revised Manuscript Received December 29, 1994[⊗]

ABSTRACT: We have investigated the interaction of fluorescent peptide ligands with the G protein-coupled receptor NK2 using novel spectrofluorometric approaches. Several heptapeptide antagonists of structure PhCO-Xaa-Ala-D-Trp-Phe-D-Pro-Pro-Nle-NH_2 were labelled on position 1 (Xaa) with the environment-sensitive nitrobenzoxadiazole (NBD) probe, differing only in the length of the spacer between the NBD group and the peptide. Upon binding of the labelled antagonist to NK2 receptors stably expressed in Chinese hamster ovary (CHO) cells, an increase in NBD fluorescence was observed when the spacer length was less than 10 Å. Collisional quenching experiments using iodide and Co^{2+} ions were performed to define the accessibility of the NBD group on bound ligands to the solvent. By comparing ligands with spacer arms of varying lengths, we found that the binding pocket is buried at a depth of 5−10 Å. In contrast, N-terminally NBD-labelled agonists, decapeptide neurokinin A (NKA) or heptapeptide Nle^{10}-NKA[4−10], bound to the NK2 receptor were accessible to the solvent. Binding of fluorescent ligands to the NK2 receptor was accompanied by an enhancement in the fluorescence anisotropy. The changes in fluorescence properties were used to determine the kinetic parameters of antagonist binding and dissociation. These results indicate that the binding site on the NK2 receptor for the amino-terminal end of the heptapeptide antagonists is buried in the hydrophobic pocket of the receptor protein and clearly distinct from the binding site for the amino-terminal end of agonists, which is accessible to the solvent. Heptapeptide agonist and antagonist may therefore have distinct but probably overlapping binding sites. These results support recent observations suggesting that peptide agonists dock in the extracellular regions of seven-transmembrane receptors. The methodology described here should be of broad applicability for investigating ligand−receptor recognition.

Cellular effects of tachykinin neuropeptides are mediated by action on cell surface receptors coupled to G proteins. Three distinct receptors, NK1, NK2, and NK3, have been cloned and show selectivity for the closely related natural agonists substance P (SP),[1] neurokinin A (NKA), and neurokinin B, respectively (Nakanishi, 1991). These receptors are predicted to have seven transmembrane helical regions and belong to a large superfamily. These receptors have a greater variety of ligands including monoamines, hormones, neurotransmitters, peptides, inflammatory mediators, and other bioactive molecules (Iismaa & Shine, 1992). Whereas there is a large body of evidence indicating that monoamine ligands bind in a pocket delineated by transmembrane helices (Strader et al., 1994), the mode of recognition between peptide ligands and seven-transmembrane receptors is much less characterized (Schwartz, 1994).

The structural basis for peptide agonist recognition by the tachykinin receptors has been investigated by using both chimeric receptors and site-directed mutagenesis. These studies have shown that multiple domains are involved in determining subtype specificity, including the N-terminal segment and extracellular loops and also possibly transmembrane regions (Gether et al., 1993a; Fong et al., 1992b; Yokota et al., 1992). However, little is known about the relative importance of these residues or domains in determining binding affinity. In fact, it appears that tachykinin peptides do not interact with the same set of functional groups on their respective receptors (Fong et al., 1992a). In contrast, nonpeptide antagonists use a different binding epitope on the NK1 receptor (Gether et al., 1993b). Specific molecular interactions between CP96345 and the NK1 receptor have been mapped to His197 (Fong et al., 1993) or His265. These residues have been shown to be required for binding of nonpeptide antagonists to the NK1 receptor (Strader et al., 1994). These residues are not involved in SP binding; however, the equivalent residues in NK2 receptor (His198, His267) are required for high-affinity binding of NKA (Huang et al., 1994). There is virtually no information available regarding recognition of peptide antagonists by tachykinin receptors.

The use of fluorescent ligands to investigate ligand−receptor interactions has proven to be a valuable complement to receptor mutagenesis studies (Tota & Strader, 1990). The physical nature of the microenvironment of the formyl

* Corresponding author; FAX +41 22 794 6965.
‡ Glaxo Institute for Molecular Biology.
§ EPFL, Ecole Polytechnique Fédérale Lausanne.
⊗ Abstract published in *Advance ACS Abstracts,* March 1, 1995.
[1] Abbreviations: CHO, Chinese hamster ovary; NBD, 7-nitrobenz-2-oxa-1,3-diazol-4-yl; SP, substance P; NKA, neurokinin A; PBS, phosphate-buffered saline; BSA, bovine serum albumin; RP-HPLC, hydrophobic interaction ("reverse-phase") high-performance liquid chromatography; DMF, *N,N*-dimethylformamide; TFA, trifluoroacetic acid; ANT, antagonist; AGO, agonist; Dab, 2,4-diaminobutyric acid; Orn, ornithine; Dap, 2,3-diaminopropionic acid; Ph, phenyl; Nle, norleucine; Su, succinimidyl; Boc, *t*-butyloxycarbonyl; Fmoc, 9-fluorenylmethyloxycarbonyl; FLU, fluoresceinthiocarbamyl.

0006-2960/95/0434-3972$09.00/0

Compound	Structure [a]	pK$_i$ [b] (n)
GR94800	PhCO-Ala-Ala-D-Trp-Phe-D-Pro-Pro-Nle-NH2	9.81 ± 0.07 (8)
ANT-1	PhCO-**Dab(γ-NBD)**-Ala-D-Trp-Phe-D-Pro-Pro-Nle-NH2	8.87 ± 0.11 (5)
ANT-2	PhCO-**Orn(δ-NBD)**-Ala-D-Trp-Phe-D-Pro-Pro-Nle-NH2	8.84 ± 0.07 (4)
ANT-3	PhCO-**Lys(ε-NBD)**-Ala-D-Trp-Phe-D-Pro-Pro-Nle-NH2	8.83 ± 0.06 (3)
ANT-4	PhCO-**Lys(ε-GlyNBD)**-Ala-D-Trp-Phe-D-Pro-Pro-Nle-NH2	8.80 ± 0.03 (3)
ANT-5	PhCO-**Lys(ε-ahNBD)**-Ala-D-Trp-Phe-D-Pro-Pro-Nle-NH2	8.62 ± 0.17 (3)
ANT-6	PhCO-**Lys(ε-bahNBD)**-Ala-D-Trp-Phe-D-Pro-Pro-Nle-NH2	8.32 ± 0.02 (2)
NKA	His-Lys-Thr-Asp-Ser-Phe-Val-Gly-Leu-Met-NH2	8.92 ± 0.04 (6)
AGO-1	**N-α (NBD)** Asp-Ser-Phe-Val-Gly-Leu-Nle-NH2	8.08 ± 0.09 (3)
AGO-2	**N-α (FLU)** Asp-Ser-Phe-Val-Gly-Leu-Nle-NH2	6.51 ± 0.20 (3)
AGO-3	**N-α (NBD)** His-Lys-Thr-Asp-Ser-Phe-Val-Gly-Leu-Met-NH2	8.23 ± 0.01 (2)
AGO-4	**N-α (FLU)** His-Lys-Thr-Asp-Ser-Phe-Val-Gly-Leu-Met-NH2	8.80 ± 0.15 (3)
AGO-5	Ac-Asp-Ser-Phe-**Dap(β-NBD)**-Gly-Leu-Nle-NH2	5.71 ± 0.05 (3)

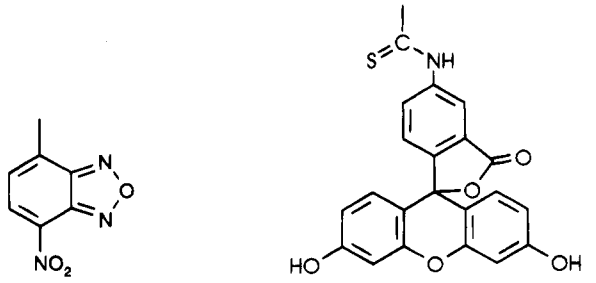

FIGURE 1: Chemical structure and binding activity of fluorescent ligands. [a]*Ac* = acetyl; ah = 6-aminohexanoyl; bah = bis(6-aminohexanoyl). [b]*Competition* for [^{3}H]GR100679 binding in CHO/T cells. pK_i values were calculated as described under Materials and Methods. Data are mean ± SE. *n* represents the number of separate assays performed in triplicate.

peptide (fMLP) receptor binding pocket was probed by studying the pH sensitivity of fluorescein-labelled peptide ligand (Fay et al., 1993). Recently, we designed and developed fluorescent agonist and antagonist ligands for the NK2 receptor: fluorescein-labelled NKA, as a biologically active probe for NK2 receptors (Ceszkowski & Chollet, 1992), and NBD-labelled heptapeptide antagonists (Bradshaw et al., 1994).

Here we report the use of spectrofluorometric methods to study the interaction of these fluorescent antagonist or agonist peptide ligands with the NK2 receptor in transfected cell lines. Using an environmentally sensitive fluorescent probe and quenching experiments, we demonstrate that the ligand binding site on the NK2 receptor for heptapeptide antagonists is in a hydrophobic pocket, shielded from the solvent, whereas the agonist binding site is accessible to the solvent. These results support the idea that agonist binding determinants are located in the extramembraneous regions of the receptor. The methodology described here should prove of general use for characterizing ligand−receptor interactions and mapping subdomains of binding sites.

MATERIALS AND METHODS

Synthesis of Fluorescent Ligands. The compounds listed in Figure 1 were prepared according to the general methods previously reported (Bradshaw et al., 1994) with the following modifications: ANT-4 was obtained by adding Boc-Gly-OSu (54 mg, 0.2 mmol) to a solution of PhCO-Lys-Ala-D-Trp-Phe-D-Pro-Pro-Nle-NH_2 (20 mg, 0.02 mmol) in 1.4 mL of 0.05 M aqueous sodium borate, pH 9.5−DMF (1:1) at 4 °C and stirring until dissolution was complete. A solution of HOBt (18 mg) in 0.1 mL of DMF was added and the mixture was stirred overnight at ambient temperature. The Boc-protected intermediate was purified by RP-HPLC. The Boc protecting group was removed by resuspending 10 mg of the intermediate in 1 mL of ice-cold TFA and incubating at room temperature for 45 min without further stirring. Approximately half of the TFA was removed by evaporation with a stream of nitrogen gas, and the deprotected peptide was recovered by precipitation with *t*-butyl methyl ether. The precipitate was subsequently resuspended in 0.1% TFA/H_2O and purified by preparative RP-HPLC. The NBD group was attached as described (Bradshaw et al., 1994). ANT-5 was prepared by coupling of NBD to the peptide PhCO-Lys(ε-ah)-Ala-D-Trp-Phe-D-Pro-Pro-Nle-NH_2, which was synthesized according to general procedures: 6-aminohexanoic acid was coupled sequentially as the Fmoc derivative, following α-benzoyl(ε-Fmoc)lysine. The overall yield was 38%. ANT-6 was synthesized by coupling of 6-NBD-aminohexanoic acid *N*-hydroxysuccinimide ester to the peptide PhCO-Lys(ε-ah)-Ala-D-Trp-Phe-D-Pro-Pro-Nle-NH_2 according to the protocol described earlier (Bradshaw et al., 1994).

Binding Assays. Radioligand binding assays on whole CHO cells transfected with NK2 receptors were perfomred in 24-well plates with 2.5 × 10^5 cells/well in a total volume of 0.5 mL of binding assay medium comprising assay buffer [50 mM Tris-HCl, pH 7.4, 100 mM NaCl, 2 mM $MgCl_2$, and 0.02% (w/v) bovine serum albumin], 1.3 nM [^{3}H]-GR100679 (cyclohexylcarbonyl-Gly-Ala-D-Trp-Phe-NMe_2) (Smith *et al.*, 1993) and varying concentrations of the test compound (10 pM−10 μM). The plates were incubated at 20 °C for 90 min and then washed three times with ice-cold assay buffer. Optiphase Hi-load (1 mL) was added to each well and the plate was counted on a microbeta scintillation counter. Nonspecific binding was determined in the presence of 1 μM GR94800 (Figure 1) (McElroy et al., 1992). All measurements were done in triplicate. Data were analyzed using Allfit and IC_{50} values converted to pK_i values (−log of the inhibition constant K_i) using the Cheng−Prusoff equation:

$$K_i = IC_{50}/1 + ([L]/K_D) \quad (1)$$

where IC_{50} is the concentration of competing ligand which displaces 50% of the specific binding of the radioligand, [L] is the concentration of the radioligand, and K_D is the dissociation constant of the radioligand for the receptor.

Cell Culture. Two CHO cell lines stably expressing the NK2 receptor were used in this study: CHO/T cells (about 4 × 10^4 receptors/cell) and CHO/A cells (about 7 × 10^5 receptors/cell) (Turcatti et al., 1993). All cells were cultured as monolayers in a humidified 5% CO_2 atmosphere at 37 °C. CHO/T cells were cultured in DMEM/F12 medium supplemented with 10% fetal calf serum, 2% (w/v) Pen-Strep, and 0.5% (w/v) Nystatin. CHO/A cells were cultured in the same medium containing 0.1 μM methotrexate. For experiments with CHO/A cells in suspension, cells were cultured as described above to 80% confluence and harvested with PBS containing 1 mM EDTA and washed with ice-cold PBS.

Spectroscopy. UV−visible absorbance spectroscopy measurements were made using a Hewlett-Packard 8452A diode array spectrophotometer at ambient temperature. Steady-state fluorescence measurements were recorded using a Jasco

FP-777 spectrofluorometer with a 0.5- × 1.0-cm quartz cuvette with 0.5 mL sample volume, stirred continuously with a magnetic bar. Unless stated otherwise, fluorescence measurements were made on suspended cells at 20 °C. The excitation wavelength was 475 nm and the emission was recorded at either 540 nm (NBD) or 520 nm (fluorescein). The excitation and emission bandwidths were 5 and 10 nm, respectively.

Collisional Quenching Experiments. About 10^6 cells were incubated in PBS, pH 7.2, containing $MgCl_2$ (3 mM) and BSA (0.2 mg/mL), in the presence of 20 nM fluorescent ligand at 20 °C for 1 h. Cells were then washed twice with ice-cold PBS, pH 7.2, and resuspended in PBS for fluorometry measurements. Fluorescence collisional quenching experiments with iodide were performed by adding increasing amounts of a 0.153 M KI solution in water to a final concentration of 50 mM in a cuvette containing an initial volume of 500 μL of suspended cells (at a density of 2−4 × 10^6 cells/mL or 2−4 nM [^{3}H]GR94800 binding sites). For Co^{2+} quenching, 50 mM $CoCl_2$ was added to CHO/A cells suspended in 20 mM sodium Hepes, pH 7.4, and 0.13 M NaCl. Changes in fluorescence due to the addition of quencher were corrected by subtracting the fluorescence measured in parallel samples in which quencher was added to cells in PBS or cells saturated with an excess (500−1000-fold) of nonfluorescent antagonist GR100679 before exposure to the fluorescent ligand. Moreover, in quenching experiments with Co^{2+}, the fluorescence was corrected for the inner filter effect as described (London, 1986). The quenching of the fluorescence emission at 540 nm was calculated with the Stern−Volmer equation (Lakowicz, 1983):

$$F_0/F = 1 + K_{sv}[I^-] \quad (2)$$

where F_0/F is the ratio of fluorescence intensities in the absence and presence of iodide. The Stern−Volmer quenching constant K_{sv} was determined from the slope of F_0/F as a function of the iodide concentration [I^-].

Real-Time Monitoring of Ligand Binding to NK2 Receptor. About (1−2) × 10^6 CHO/A cells were suspended in 500 μL of PBS containing 3 mM $MgCl_2$ and 20 mg/mL BSA at 20 °C (about 1−2 nM [^{3}H]GR94800 binding sites). Fluorescence binding measurements were initiated by addition of 10 nM fluorescent antagonist ANT-1. The binding was monitored on the spectrofluorometer at 540 nm. After completion of binding (constant value of fluorescence emission), a 500-fold molar excess of the antagonist competitor GR100679 or GR94800 was added and dissociation of ANT-1 was monitored over time. Contribution due to free ligand was subtracted by comparison with samples preincubated with 5 μM GR100679. Radiolabeled binding experiments were initiated by addition of 1 nM [^{3}H]-GR94800. Time points were taken from 2 to 120 min. The cells were pelleted by quick centrifugation in a microfuge, washed twice with ice-cold PBS, and counted. Dissociation of radiolabeled [^{3}H]GR94800 was performed with cells incubated with 1 nM GR94800 for 1 h at 20 °C. After two washes with ice-cold PBS, the dissociation was initiated by addition of 1 μM GR100679. Time points from 2 to 90 min were taken and cells were counted after two washes with ice-cold PBS. Rate constants for association (k_{ass}) and the observed pseudo-first-order rate constants (k_{obs}) were calculated from

$$k_{obs} = k_{ass}[L] + k_{diss} = (\ln [B_{eq}/(B_{eq} - B_t)])/t \quad (3)$$

where B_{eq} is the fraction bound at equilibrium, B_t is the fraction bound at time t during the association, and [L] is the ligand concentration. Dissociation rate constants (k_{diss}) were obtained from

$$k_{diss} = \ln (B_t/B_0)/t \quad (4)$$

where B_t is ligand bound at time t and B_0 is ligand bound at time $t = 0$ (Limbird, 1986).

Fluorescence Anisotropy Measurements. Steady-state anisotropy measurements were recorded using a Jasco FP-777 spectrofluorometer equipped with a Model ADP-301 fluorescence polarization accessory. The polarizer and analyzer were placed in the thermostatic sample chamber. The emission intensity was measured by setting the excitation-side polarizer in the vertical position (V) and the emission-side polarizer in either the horizontal (H) or vertical position. The emission intensities, in respective V and H positions, were corrected by subtracting the corresponding background signals from the cells or membrane suspensions and converted to anisotropy (A) with

$$A = [[(I_V/I_H)/G] - 1]/[[(I_V/I_H)/G] + 2] \quad (5)$$

where I_V/I_H is the ratio of the vertical and horizontal emission intensities when the excitation polarizer is in the vertical position and G is the same ratio when the excitation light is horizontally polarized. Binding of fluorescent ligands to NK2 in CHO cells was made as described above. The limiting anisotropy A_0 in the absence of rotation and the rotation correlation times (ϕ) were calculated with the Perrin equation for the case of a spherical molecule (Lakowicz, 1983):

$$A^{-1} = A_0^{-1}(1 + \tau/\phi) = A_0^{-1}(1 + \tau kT/V_h\eta) \quad (6)$$

where τ is the fluorescence lifetime of the NBD chromophore attached to the peptide, k is Boltzmann's constant, T is the temperature, V_h is the partial molecular volume of a hydrated sphere, and η is the viscosity. Perrin plots were constructed by measuring anisotropy of ANT-1 free, 20 nM in PBS solution, or bound to membranes from CHO/A cells, as a function of either temperature over a range of 2−37 °C or viscosity by addition of increasing amounts of glycerol (0−80% w/v) at constant 20 nM concentration of ANT-1. The viscosity at each temperature was determined from standard tables (Weast, 1980).

RESULTS AND DISCUSSION

Synthesis of Fluorescent Ligands. We have designed and prepared a series of fluorescence-labelled heptapeptide antagonists to the NK2 receptors (Figure 1). The antagonists ANT-1−ANT-6 differ in the length of the spacer arm linking the fluorescent probe to the peptide. Fluorescent antagonists were derived from the potent and selective ligand GR94800 (McElroy et al., 1992), in which Ala1 was replaced by Dab or Orn or Lys, respectively, and the newly introduced side-chain amino group was derivatized with the fluorescent group 7-nitrobenz-2-oxa-1,3-diazol-4-yl (NBD) to give the homologous compounds ANT-1, ANT-2 or ANT-3, respec-

Table 1: Distance between the NBD Group and the Peptide in Fluorescent Antagonists

compound	d^a (Å)	compound	d^a (Å)
ANT-1	4	ANT-4	10
ANT-2	5	ANT-5	15
ANT-3	6.5	ANT-6	24

[a] *d* represents the extended distance between the NBD group and the Cα of the amino acid at position 1.

tively (Bradshaw et al., 1994). Ligands with longer tethers (ANT-4, ANT-5, and ANT-6) were synthesized by attaching the NBD group to a lysyl group extended with glycyl, aminohexanoyl, or bis(aminohexanoyl) linkers, respectively. The linearized lengths of the spacing arms between the Cα at position 1 in the peptide and the NBD group span distances from approximately 4 Å for ANT-1 to 24 Å for ANT-6 (Table 1).

Three reasons led to the choice of NBD as a fluorescent probe. First, the NBD group has a relatively small molecular volume and was predicted to have minimal perturbation on the affinity of the heptapeptide for the NK2 receptor. Second, NBD has favorable absorbance and fluorescence properties, and third, its fluorescence is strongly sensitive to the medium, with higher fluorescence in a hydrophobic environment.

Biological activity of peptides ANT-1−ANT-6 was assessed by competitive displacement binding assay with the NK2-selective antagonist [^{3}H]GR100679 (Smith et al., 1993). Compared to the potent parent peptide GR94800, the fluorescent peptides ANT-1−ANT-6 maintained a high affinity for the NK2 receptor with only an 8−30-fold decrease in affinity (Figure 1). ANT-1−ANT-6 have been shown to be antagonists in a functional NK2 assay (Bradshaw et al., 1994).

Fluorescent decapeptide agonists were synthesized by selective labelling of NKA at the Nα-amino group of His1. The NBD-labelled AGO-3 was obtained by reaction of NKA with 1 equiv of NBD fluoride in sodium borate buffer at pH 9.5. Under these conditions only the Nα-amino group of His1 was derivatized as shown by Edman degradation (Ceszkowski & Chollet, 1992). Fluorescein-labelled NKA (AGO-4) was prepared as reported earlier (Ceszkowski & Chollet, 1992). The fluorescent heptapeptides AGO-1 and AGO-2 were made by the same method starting from the heptapeptide Nle^{10}-NKA[4−10] (Rovero et al., 1989). The ligands AGO-1, AGO-3, and AGO-4 conserved a relatively high affinity for the NK2 receptor compared to the natural ligand NKA, whereas ligand AGO-2 was much less potent. AGO-1−AGO-4 activate the NK2 receptor in transfected CHO cells as assayed by Ca^{2+} mobilization assay. This activity was blocked by the selective NK2 antagonist GR94800. This indicates that the tagging of NKA or Nle^{10}-NKA[4−10] has not impaired their agonistic activity. AGO-5 differed from Nle^{10}-NKA[4−10] in that Val^7 was replaced by (L)-diaminopropionic acid (Dap), which was derivatized by NBD on the side-chain amino group. Affinity of AGO-5 for the NK2 receptor was strongly reduced, indicating that unfavorable steric or electronic interactions occur between NBD and residues in the binding pocket.

All peptides were purified by hydrophobic interaction chromatography (reverse-phase HPLC) and characterized by electrospray mass spectrometry and amino acid analysis.

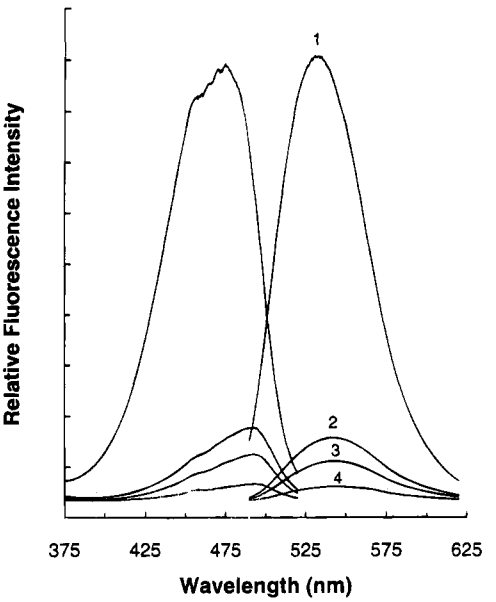

FIGURE 2: Excitation and emission spectra of NBD ligand ANT-1 (1 μM) in solvents of different polarity: 1 = 90% dioxane in water (v/v); 2 = 10% dioxane in water; 3 = 5% dioxane in water; 4 = PBS, pH 7.2.

Fluorescence Properties of NBD Ligands. The excitation and emission maxima of NBD ligands in PBS, pH 7.2, are 492 ± 2 and 540 ± 2 nm, respectively. The molar extinction coefficient (ε) of ANT-1 at 20 °C in methanol is 30 900 M^{-1} cm^{-1} at 466 nm, based on quantitative amino acid analysis of the fluorescent peptide using Leu as internal standard (Allen, 1981). The quantum yield of NBD is dependent upon the polarity of the environment, with a higher quantum yield in a low-polarity environment (Lancet & Pecht, 1977). This property has been utilized to study the environment of the ribosome−nascent chain−membrane complexes using NBD incorporated into the signal sequence (Crowley et al., 1993). To evaluate the utility of NBD as a probe for the polarity of the surrounding medium, the emission of ANT-1 was examined in solvents of different polarities (Figure 2). For ANT-1, the emission maximum shifted from 540 to 530.5 nm and the emission intensity increased 30-fold when going from an aqueous (PBS) to a less polar solvent (e.g., chloroform). Fluorescence in PBS increased linearly as a function of ligand concentration in the presence or absence of cells containing a 1000-fold excess of competitor antagonist GR100679 over NK2 binding sites.

Interactions of the Fluorescent Ligands with NK2 Receptor on CHO Cells. Binding of fluorescent NBD ligands to the NK2 receptor was measured on a suspension of transfected CHO cells expressing about 7 × 10^5 NK2 receptors/cell (Turcatti et al., 1993). Figure 3 shows a typical fluorescence emission spectrum for ANT-1. The quantum yield of NBD fluorescence emission increased about 5-fold when the antagonist ligand ANT-1 or ANT-2 was found to the NK2 receptor on transfected CHO cells, indicating that the fluorophore in the receptor-bound state was in a less polar environment than in the unbound state. Our interpretation is that the hydrophobicity around the fluorescent reporter has increased. A similar fluorescence intensity increase as in the case of receptor binding can be obtained by dissolving ANT-1, AGO-1, or AGO-3 in a 5% (v/v) dioxane mixture in water. The intensity and the quantum yield of NBD fluorescence emission for ANT-1 in PBS buffer were not

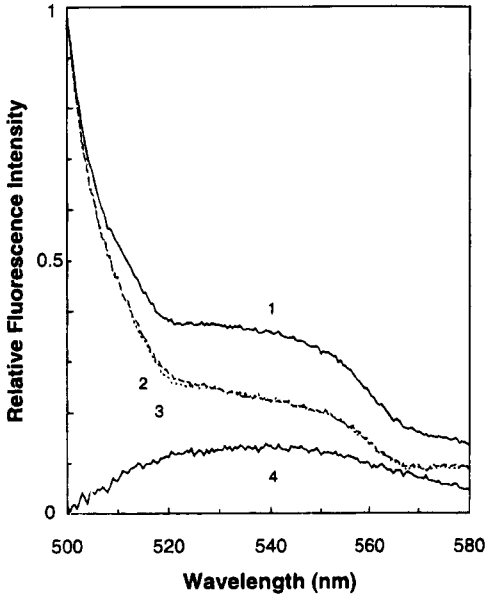

FIGURE 3: Spectrofluorometric analysis of binding of fluorescent heptapeptide antagonist ANT-1 to NK2 receptors on CHO/A cells. Excitation at 475 nm. 1 = fluorescence in presence of 20 nm ANT-1; 2 = fluorescence in presence of 20 nM ANT-1 and 20 μM GR100679; 3 = autofluorescence of the cells in the absence of ligand; 4 = specific fluorescence (difference spectrum 1 − 2).

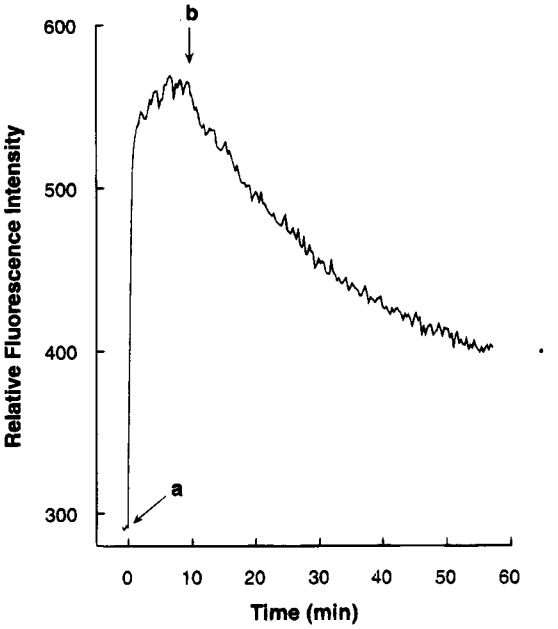

FIGURE 4: Real-time monitoring of ANT-1 ligand binding to NK2 receptors on CHO/A cells at 540 nm. (a) Addition of 10 nM ANT-1; (b) addition of 5 μM GR94800.

changed in the presence of CHO cells expressing no NK2 receptors or in the presence of CHO/A cells containing a large molar excess (10 μM) of the NK2 antagonist GR100679. Smaller increases in fluorescence were also observed for ligands ANT-3 and ANT-4, whereas the fluorescence emission for ANT-5 and ANT-6 was unchanged compared to that of the free ligand in solution. In contrast, there was no increase in quantum yield of fluorescence emission for NBD-labelled agonists (AGO-1 and AGO-3) when they were allowed to bind to NK2 receptor, suggesting that the polarity of the binding pocket for the N-terminal portion of agonists was similar to that of the aqueous solution. The specific fluorescence of fluorescein-labelled agonists AGO-2 and AGO-4 bound to NK2 was much brighter than for AGO-1 and AGO-3, though AGO-2 and AGO-4 have lower binding affinity. Similar results were obtained by flow cytometry (data not shown). This indicates that the weak fluorescence signal observed for bound NBD agonists is principally due to quenching in the polar environment. Taken together, these data suggest that the environment around the amino-terminal end of ligands bound to NK2 is more hydrophobic for antagonists than for agonists.

Kinetics of Ligand Binding and Dissociation. Fluorescent-labeled ligands may serve as probes for receptor binding (Carraway & Cerione, 1993). We monitored the binding of the NBD-containing antagonist ligand ANT-1 to the NK2 receptor in real time and its dissociation after addition of an excess of competitive antagonist. Figure 4 shows the fluorescence at 540 nm as a function of time when 10 nM ANT-1 was added to suspended CHO/A cells in the absence or presence of an excess of NK2 antagonist GR94800. There was a rapid increase in fluorescence due to specific binding to NK2 receptors, and equilibrium was reached after about 5−6 min. No specific binding was observed in the presence of an excess of competitive antagonist. The kinetic parameters are listed in Table 2. The observed pseudo-first-order

Table 2: Kinetics of Binding of Ligands to CHO/NK2 Cells

	ligand association		ligand dissociation			
ligand	k_{obs} (min^{-1})	[n]	$k_{diss}1$ (min^{-1})	[n]	$k_{diss}2$ (min^{-1})	[n]
[^{3}H]GR94800	0.37 ± 0.08	[2]	0.036 ± 0.005	[3]	0.005 ± 0.003	[3]
ANT-1	0.53 ± 0.10	[4]	0.022 ± 0.006	[3]	0.006 ± 0.002	[3]

rate constant of association (k_{obs}) was calculated from eq 3. A linear plot was obtained ($r = 0.97$) from which a value of $k_{obs} = 0.53 \pm 0.1$ min^{-1} was calculated. The half-time for association was then calculated to be 1.4 min. These values were similar to the kinetics of [^{3}H]GR94800 binding to CHO/A cells (Table 2). An association rate constant $k_{ass} = 5.1 \times 10^7$ min^{-1} M^{-1} was calculated from eq 3. The binding was reversible; addition of an excess of the competitive antagonist GR100679 caused a slow decrease in affinity explained by dissociation of ANT-1 from NK2 receptor. The linear transformation of dissociation data using eq 4 was best fitted with a biphasic curve with $k_{diss} = 0.022$ min^{-1} and 0.006 min^{-1}. The dissociation constant (K_D) calculated from the association and initial dissociation rate data was 0.43 nM for ANT-1 binding to NK2 receptor, a value similar to the K_D for the agonist ^{125}I-neuropeptide γ (Takeda et al., 1992). In summary, the change in fluorescence emission intensity was monitored in real time, making possible the determination of kinetic constants for the association and dissociation of ANT-1. The association was quite rapid. The dissociation was biphasic, a feature that had been reported before for tachykinins (Guard *et al.*, 1990). However, this does not indicate binding to two different sites since saturation binding analysis with the heptapeptide [^{3}H]-GR94800 revealed only one site (Turcatti et al., 1993). Alternatively, the secondary, slower dissociation phase may indicate possible association of the hydrophobic ligand with the membrane. In the future, rapid kinetic experiments using stopped-flow techniques could allow one to measure association with a higher resolution and therefore possibly differentiate between an initial membrane association and a subsequent receptor binding phase.

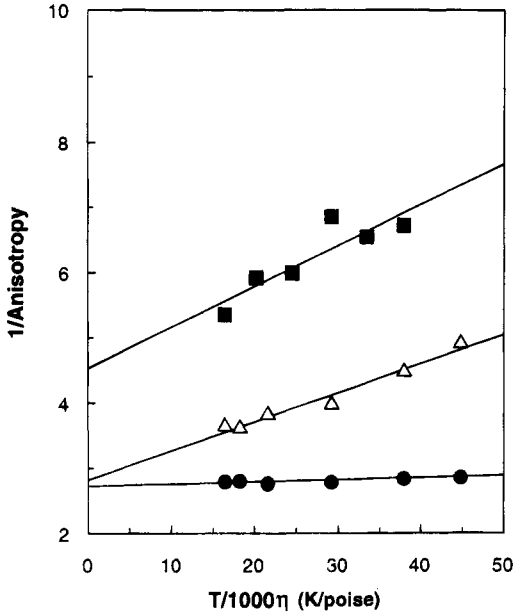

FIGURE 5: Perrin plots (cf. eq 6) of ANT-1 free, 20 nM in PBS solution (■), free in PBS in the presence of CHO cells (△), and bound to NK2 receptors on CHO/A cells (●).

Fluorescence Anisotropy Measurements. The fluorescence anisotropy of a chromophore attached to macromolecules in general and to peptides in particular reflects directly the molecular mobility of the fluorescent reporter group. In our present case, the mobility of the peptide ligands will, upon binding to membrane receptors, be considerably restricted as compared to the free state in solution. In principle, the mobility of the ligand-attached fluorophore will to a certain extent reflect the mobility of the receptor or the ligand binding site of the receptor, the internal mobility of the ligand, and finally the motional freedom of the chromophore relative to the ligand molecule. These different kind of motions are expected to occur in different time regimes and might be distinguished by time-resolved fluorescence anisotropy measurements to a certain extent, depending on the fluorescence lifetime of the chromophore (Szabo, 1984). It is the sum of all these effects which finally influences the steady-state fluorescence anisotropy. In particular, the relative mobility of the chromophore versus the peptide ligand molecule will determine the extent of the steady-state fluorescence anisotropy change upon receptor binding.

The Perrin plot of the free peptide ANT-1 (20 nM) in buffer (Figure 5) shows two important results. First, the extrapolated value of $A_0 = 0.22$ is considerably lower than that of a totally immobilized ligand with $A_0 = 0.4$ (see below). This indicates a relatively high mobility of the NBD fluorophore relative to the peptide molecule. Second, from the slope of the Perrin plot one calculates a rotational correlation time of $\phi \cong 2.5$ ns for the peptide molecules, assuming a typical fluorescence lifetime of $\tau \cong 1$ ns for water-accessible groups (Crowley et al., 1993; unpublished results). This in turn corresponds to a relative molecular mass of $M \cong 6000$ for the peptide molecules in aqueous medium, compared to a calculated $M = 1096$ for ANT-1, indicating the presence of peptide aggregates on the order of pentamers or hexamers.

Anisotropy of Fluorescent Ligands Increases upon Binding to NK2 on CHO/A Cells. The binding of the heptapeptide ligands to NK2 receptors on CHO/A cells considerably increases the NBD anisotropy compared to that of the peptides in solution (Table 3). Limiting values of A_0 ranging from 0.36 to 0.4 can be calculated for ANT-1−ANT-6 when bound to NK2 receptors. These values can only be calculated approximately, as they were derived from Perrin plots in which τ and η values are assumed to be the same as for ligands in water solution. The increase in fluorescence observed upon receptor binding and likely steric interactions of the ligands with receptors suggest that both τ and η values are to increase in the receptor-bound state. The Perrin plot for corresponding actual τ and η values of the receptor-bound ligand would not change very much because the fluorescence anisotropy values remain practically constant. The mostly temperature-insensitive high anisotropy values of the different ligands bound to the receptors, both in whole cells (Table 3) as well as in isolated membranes (data not shown), demonstrate that the ligands are nearly totally immobilized at the receptor binding site(s) in the nanosecond time range, irrespective of the length of the spacer between the peptide and the fluorophore. The high anisotropy for bound ligands could be due to immobilization of the ligands by a densely packed environment surrounding the receptor binding site or a conformational change of the peptide ligand upon binding.

Table 3: Anisotropy of Fluorescent Ligands[a]

ligand	anisotropy (n)
bound to receptors on CHO/A cells	
ANT-1	0.35 ± 0.03 (5)
ANT-2	0.38 ± 0.03 (3)
ANT-3	0.38 ± 0.02 (3)
ANT-4	0.37 ± 0.02 (5)
ANT-5	0.36 ± 0.05 (3)
in the absence of receptor binding	
ANT-1 in PBS solution	0.13 ± 0.01 (5)
ANT-1 in CHO cells[b]	0.23 ± 0.02 (3)
ANT-1 in CHO/A cells[c]	0.22 ± 0.02 (3)

[a] Binding of ligands and anisotropy measurements were made as described under Materials and Methods. [b] Nontransfected parental CHO cells in PBS buffer. [c] ANT-1 (40 nM) in suspended CHO/A cells in PBS preincubated with 4 μM GR94800.

A comparison of fluorescence anisotropy data for ANT-1 in the presence of CHO cells lacking NK2 receptors, CHO/A cells plus an excess of competitive antagonist, and free in PBS indicates a reduced mobility of the peptide ligand in presence of cells (Table 3). This reduction in mobility is not as strong as in the case of binding to the receptor ($A = 0.35$). Perrin plots show that the extrapolated values of A_0 for ANT-1 bound to NK2 receptors and for free ANT-1 in the presence of CHO cells void of receptors are practically identical (Figure 5). In contrast, the slopes of $1/A$ vs T/η for ANT-1 in PBS buffer in the presence or absence of CHO cells are nearly identical. From this we conclude that, first, the hydrophobic ligand partitions nonspecifically into the membranes, and second, the mobility of the ligand incorporated in the membrane is clearly higher than that of the receptor-bound state. The nonspecific partitioning of the peptide ligand into membranes is interesting, as it has been suggested that cell membranes may catalyze the interaction between regulatory peptides and their cell surface receptors (Sargent & Schwyzer, 1986).

Collisional Quenching Experiments. Collisional quenching of fluorescence is a powerful technique which can be used to probe solvent accessibility of receptor-bound ligand

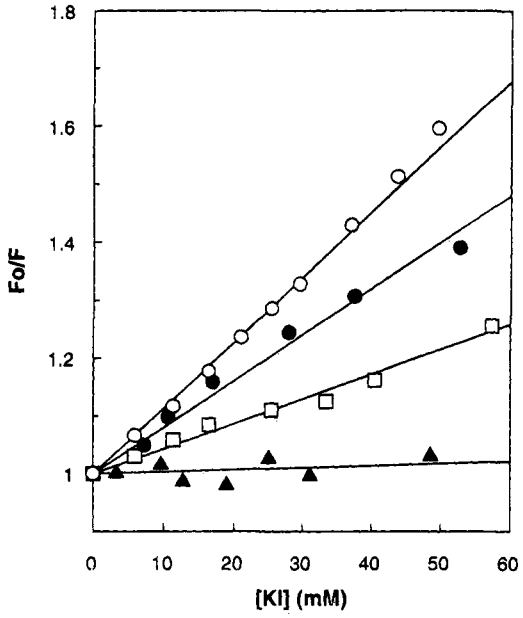

FIGURE 6: Stern–Volmer plots of F_0/F vs iodide concentration (cf. eq 4) for quenching of the fluoresecence of receptor-bound antagonist ligands by iodide. ○ = free ligands in solution; ● = ANT-5; □ = ANT-3; ▲ = ANT-1.

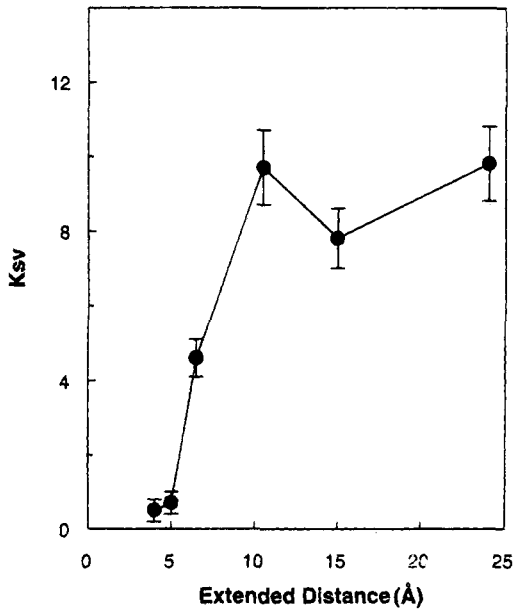

FIGURE 7: Stern–Volmer quenching constant K_{SV} as a function of spacer length (assuming an extended conformation) between NBD and the peptide of the antagonists. Lines are solely drawn to guide the eye.

Table 4: Stern–Volmer Constants of Quenching of Fluorescent NK2 Ligands by Iodide[a]

ligand	K_{SV} free (M^{-1})	K_{SV} bound (M^{-1})
ANT-1	10.9 ± 0.4	0.5 ± 0.3
ANT-2	10.8 ± 0.4	0.7 ± 0.3
ANT-3	10.7 ± 0.3	4.6 ± 0.5
ANT-4	10.7 ± 0.5	9.8 ± 1.0
ANT-5	10.8 ± 0.5	7.6 ± 0.8
ANT-6	10.7 ± 0.3	9.8 ± 1.8
AGO-2	4.2 ± 0.5	4.5 ± 0.6
AGO-4	4.5 ± 0.5	4.2 ± 0.7

[a] K_{SV} free values are average values of three or more independent experiments.

(Tota & Strader, 1990). We have used this technique to further characterize the binding pockets for agonist and antagonist peptides. The anion iodide and the cation Co^{2+} have been shown to quench NBD fluorescence (Allegrini et al., 1983; Homan & Eisenberg, 1985). The fluorescence of all NBD-labelled ligands free in solution was efficiently quenched by addition of increasing amounts of iodide to the solution. When the ionic strength of the solution was maintained at 0.153 M, a linear Stern–Volmer plot was obtained. This is indicative of collisional quenching. The Stern–Volmer constant, the slope of F_0/F as a function of iodide concentration, is a measure of the degree of exposure of the NBD group to the solvent. A comparison of Stern–Volmer constants for ligands free in solution or bound to receptor can serve as an indication of the degree to which the receptor shields the ligand from solvent. NK2 receptors on suspended CHO/A cells were saturated with fluorescent ligand, the excess of ligand was removed, and after addition of iodide, quenching was measured. Figure 6 shows the Stern–Volmer plots obtained for various NBD antagonists and Table 4 summarizes the experimental Stern–Volmer constants. Antagonist ligands ANT-1 and ANT-2 were protected from iodide quenching, indicating that the NBD group was not accessible to the solvent. In contrast, ANT-4, ANT-5, and ANT-6 were quenched by iodide with Stern–Volmer constants comparable to those of ligands free in solution, indicating that the NBD group on these ligands was fully exposed to the solvent. ANT-3 ligand was only partially quenched by iodide. Figure 7 shows the relationship between quenching and the extended distance (d) of the spacer between the NBD group and the heptapeptide backbone in antagonist ligands (Table 1). Ligands with $d \leq 5$ Å were inaccessible to iodide, whereas ligands with $d \geq 10$ Å were efficiently quenched. To rule out that lack of iodide quenching was not due to repulsion of iodide by negatively charged headgroups on membrane lipids, collisional quenching of the fluorescence of NK2-bound ligands ANT-1, ANT-2, and ANT-5 by the positively charged aqueous-phase quencher Co^{2+} was performed in Hepes/NaCl buffer. The Stern–Volmer constant for bound ANT-5 (51 ± 6 M^{-1}) was comparable to that in free solution (52 ± 1 M^{-1}) and was much higher than those for ANT-1 (16 ± 2 M^{-1}) and ANT-2 (14 ± 3 M^{-1}). Thus, quenching data using either cationic or anionic quenchers demonstrate that the NBD group on bound ANT-5 is fully exposed to the solvent whereas it is shielded on ANT-1 and ANT-2. Absolute values of Stern–Volmer constants for Co^{2+} were higher than for iodide quenching. This observation is best explained by the solvent dependence of the Co^{2+} quenching efficiency (Morris et al., 1985). Together, these data indicate that the binding pocket for heptapeptide antagonists is buried in the protein or membrane approximately 5–10 Å away from the membrane–water interface. It is surprising that the motion of the receptor-bound ligand, measured by fluorescence anisotropy (see above), is not influenced by peptide–NBD spacer lengths whereas a clear dependence is seen with respect to the chromophore accessibility by quenchers from the aqueous phase.

Because of the weak specific fluorescence signal for AGO-1 or AGO-3 in the receptor-bound state (see above), collisional quenching experiments for agonists were performed with fluorescein-labelled AGO-2 and AGO-4. As shown in Table 4, the fluoresceinyl group was quenched by

iodide with the same efficiency in the receptor-bound state or free in solution, indicating that the N-terminal part of peptide agonists bound to NK2 is fully accessible to the aqueous solvent. To probe the environment of the middle portion of the peptide agonists, we designed and prepared the fluorescent ligand AGO-5. Unfortunately, the affinity of AGO-5 for the NK2 receptor was too low for fluorescence measurements. Loss of binding affinity upon labeling is an intrinsic limitation of the fluorescence-based approach reported in this work and may preclude the physical mapping of some subdomains of the binding pocket.

Implication for Ligand−Receptor Recognition. The investigation of changes in properties of environment-sensitive fluorescent groups on ligands upon interaction with their receptors is a valuable approach to characterize binding sites. The data presented here support a model in which agonist and antagonist heptapeptides recognize binding sites on NK2 receptor that are spatially not identical and that differ in the nature of the binding determinants. The amino-terminal portion of antagonists bind into a hydrophobic pocket shielded from the solvent and located at a depth of 5−10 Å in the protein or membrane. In contrast, the amino-terminal regions of all investigated agonists bound to NK2 receptors are accessible to the solvent. Tachykinin peptides have a common C-terminal moiety of structure Phe-Xaa-Gly-Leu-Met-NH_2 and a 5−6 amino acid long divergent N-terminal moiety. A concept of "message-address" has been hypothesized for tachykinins (Schwyzer, 1977; Portoghese, 1989), with the highly conserved C-terminus being the message sequence involved in receptor activation mechanism and the variable N-terminus being the address portion responsible for receptor subtype selectivity. Our results support a model involving the extracellular regions of the receptor as the major binding determinant for the amino-terminal address region of NK2 agonist and support recent mutagenesis work on NK1 receptor that identifies peptide binding determinants in the N-terminal domain and extracellular loops (Strader et al., 1994). The engagement of extracellular portions of the receptor in ligand binding may also operate in many peptide receptors of the seven transmembrane superfamily and is supported by recent publications on formyl peptides receptors (Perez et al., 1993), NK1 receptor (Strader et al., 1994), thrombin receptors (Gerszten et al., 1994), NPY receptor (Walker et al., 1994), C5a receptor (Siciliano et al., 1994), and IL-8 receptors (Leong et al., 1994). Due to the failure to obtain high-affinity ligand fluorescently labelled at the central or C-terminal regions of tachykinins, we were unable to probe the microenvironment of the message sequence. For peptide antagonists, our data suggest that the binding site for the amino-terminal portion of the ligand is located in a region which is rich in hydrophobic residues, perhaps a pore formed by the seven helical transmembrane domains. It is also possible, however, that the binding pocket may simply be shielded by the extracellular loops connecting the helices. Further genetic and biochemical investigations will be necessary to determine if the peptide and nonpeptide antagonist binding sites are identical.

Understanding ligand−receptor recognition in G protein-coupled receptors at the molecular level will require the integration of genetic, biochemical, and biophysical approaches. The methods described here and based on spectrofluorometry techniques should prove of general applicability to obtain insights on fluorescent peptide ligands recognition and to characterize subdomains of ligand-binding sites.

ACKNOWLEDGMENT

We thank Charles Bradshaw for help with the peptide synthesis, Karin Nemeth for help with the cell culture, Dr. Mike Edgerton for critical reading of the manuscript, and Dr. Jonathan Knowles for stimulating discussions and continued support.

REFERENCES

Allegrini, P. R., Sigrist, H., Schaller, J., & Zahler, P. (1983) *Eur. J. Biochem. 132*, 603−608.
Allen, G. (1989) in *Laboratory Techniques in Biochemistry and Molecular Biology* (Burdon, R. H., & van Knippenberg, P. H., Eds.) 2nd ed., Vol. 9, p 37, Elsevier, Amsterdam.
Bradshaw, C., Ceszkowski, K., Turcatti, G.; Beresford, I., & Chollet, A. (1994) *J. Med. Chem.* 37, 1991−1995.
Carraway, K. L., & Cerione, R. A. (1993) *Biochemistry 32*, 12039−12045.
Ceszkowski, K., & Chollet, A. (1992) *Bioorg. Med. Chem. Lett. 6*, 609−612.
Corwley, K. S., Reinhart, G. D., & Johnson, A. E. (1993) *Cell 73*, 1101−1115.
Fay, S. P., Domalewski, M. D., & Sklar, L. A. (1993) *Biochemistry 32*, 1627−1631.
Fong, T. M., Huang, R. R. C., & Strader, C. D. (1992a) *J. Biol. Chem. 267*, 25664−25667.
Fong, T. M., Yu, H., Huang, R. R. C., & Strader, C. D. (1992b) *Biochemistry 31*, 11806−11811.
Fong, T. M., Cascieri, M. A., Yu, H., Bansal, A., Swain, C., & Strader, C. D. (1993) *Nature 362*, 350−353.
Gerszten, R. E., Chen, J., Ishii, M., Ishii, K., Wang, L., Nanevicz, T., Turck, C. W., Vu, T. K. H., & Coughlin, S. R. (1994) *Nature 368*, 648−651.
Gether, U., Johansen, T. E., & Schwartz, T. W. (1993a) *J. Biol. Chem. 268*, 7893−7898.
Gether, U., Johansen, T. E., Snider, R. M., Lowe, J. A., III, Nakanishi, S., & Schwartz, T. W. (1993b) *Nature 362*, 345−348.
Guard, S., Watson, S. P., Maggio, J. E., Phon-Too, H., & Watling, K. J. (1990) *Br. J. Pharmacol. 99*, 767−773.
Homan, R., & Eisenberg, M. (1985) *Biochim. Biophys. Acta 812*, 485−492.
Huang, R. R. C., Yu, H., Strader, C. D., & Fong, T. M. (1994) *Biochemistry 33*, 3007−3013.
Iisma, T. P., & Shine, J. (1992) *Curr. Opin. Cell Biol. 4*, 195−202.
Lakowicz, J. R. (1983) *Principles of Fluorescence Spectroscopy*, pp 131−135, Plenum Press, New York.
Lancet, D., & Pecht, I. (1977) *Biochemistry 16*, 5150−5157.
Leong, S. R., Kabakoff, R. C., & Hébert, C. A. (1994) *J. Biol. Chem. 269*, 19343−19348.
Limbird, L. E. (1986) in *Cell Surface Receptors: A Short Course on Theory and Methods*, pp 88−94, Martinus Nijhoff Publishing, Boston, MA.
London, E. (1986) *Anal. Biochem. 154*, 57−63.
McElroy, A. B., Clegg, S. P., Deal, M. J., Ewan, G. B., Hagan, R. M., Ireland, S. J., Jordan, C. C., Porter, B., Ross, B. C., Ward, P., & Whittington, A. R. (1992) *J. Med. Chem. 35*, 2582−2591.
Morris, S. J., Bradley, D., & Blumenthal, R. (1985) *Biochim. Biophys. Acta 818*, 365−372.
Nakanishi, S. (1991) *Annu. Rev. Neurosci. 14*, 123−126.
Perez, H. D., Holmes, R., Vilander, L. R., Adams, R. R., Manzana, W., Jolley, D., & Andrews, W. H. (1993) *J. Biol. Chem. 268*, 2292−2295.
Portoghese, P. S. (1989) *Trends Pharmacol. Sci. 10*, 230−235.
Rovero, P., Pestellini, V., Rhaleb, N.-E., Dion, S., Rouissi, N., Tousignant, C., Telemaque, S., Drapeau, G., & Regoli, D. (1989) *Neuropeptides 13*, 263−270.
Sargent, D. F., & Schwyzer, R. (1986) *Proc. Natl. Acad. Sci. U.S.A. 83*, 5774−5778.
Schwartz, T. W. (1994) *Curr. Opin. Biotechnol. 5*, 434−444.

Schwyzer, R. (1977) *Ann. N.Y. Acad. Sci. 297*, 3−26.
Siciliano, S. J., Rollins, T. E., DeMartino, J., Konteatis, Z., Malkowitz, L., Van Riper, G., Bondy, S., Rosen, H., & Springer, M. S. (1994) *Proc. Natl. Acad. Sci. U.S.A. 91*, 1214−1218.
Smith, P. W., McElroy, A. B., Pritchard, J. M., Deal, M. J., Ewan, G. B., Hagan, R. M., Ireland, S. J., Ball, D., Beresford, I., Sheldrick, R., Jordan, C. C., & Ward, P. (1993) *Bioorg. Med. Chem. Lett. 3*, 931−936.
Strader, C. D., Fong, T. M., Tota, M. R., Underwood, D., & Dixon, R. A. F. (1994) *Annu. Rev. Biochem. 63*, 101−132.
Szabo, A. (1984) *J. Chem. Phys. 81*, 150−167.
Takeda, Y., Blount, P., Sachais, B. S., Hershey, A. D., Raddatz, R., & Krause, J. E. (1992) *J. Neurochem. 59*, 740−745.
Tota, M. R., & Strader, C. D. (1990) *J. Biol. Chem. 265*, 16891−16897.
Turcatti, G., Ceszkowski, K., & Chollet, A. (1993) *J. Receptor Res. 13*, 639−652.
Walker, P., Munoz, M., Martinez, R., & Peitsch, M. C. (1994) *J. Biol. Chem. 269*, 2863−2869.
Weast, R. C., Ed. (1980) *Handbook of Chemistry and Physics*, 61st ed., p F-51, CRC Press, Boca Raton, FL.
Yokota, Y., Akazawa, C., Ohkubo, H., & Nakanishi, S. (1992) *EMBO J. 11*, 3585−3591.

BI942599J